Simulation of experimental diagnostics, An investigative tool for MHD instabilities

J. Manickam
Princeton Plasma Physics Laboratory
Box 451, Princeton N.J. 08543

Abstract

Mode identification of MHD instabilities observed in a plasma discharge is often based on modeling experimental signals, from a variety of diagnostics, including Mirnov loops, electron cyclotron emission, the motional Stark effect, MSE, diagnostic and measurements of soft X-ray emission. The data is compared with theoretical models of instabilities determined from representative equilibria. This process of comparison is often tedious and not always conclusive. We have developed a suite of tools to facilitate comparison of each of these diagnostics based on the predicted mode structure for global instabilities as obtained from PEST. Comparisons with experiment for a variety of instabilities will be presented.

This work supported by US Department of Energy under contract No. DE-AC02-76-CHO-3073

Experiment and Theory have different perspectives

- Magnetic coordinates Ψ,θ,ϕ
- Single mode
- Displacement vector
- Perturbed field
- Normalization – B=1
- Fourier representation

- Cartesian coordinates
- X,Y,Z
- δn, δT, emissivity
- Multiple-modes
- Nonlinear
- Power spectrum
- impurities

Comparison of theory and experiment

- Parametric dependence
  - Stability limits
  - min-q ~ 1
- Mode frequency - rotation
- Mode number – odd/even
- Radial structure

Very few detailed comparisons

Diagnostics' features

- Mirnov loops
- ECE electron cyclotron emission
- MSE – motional Stark effect
- X-ray emission
- Firetip - far-infrared, tangential interferometer/polarimeter

ξ, B – F(ψ,θ,ϕ) – External

ξ – Internal

B, n – Internal

n, T, ξ, Internal – global

n_e, B - internal

Simulation Model

- Experimental profiles for equilibrium
- Stability analysis – n, boundary conditions
- Postprocessor to determine perturbed fields, density and temperature
- Synthetic diagnostics to mimic experiment

Model for mode

- MHD time scale is ~ 1-10 microseconds
- Challenging for measurement
  - Linear phase is brief – look at nonlinear
- Treatment of nonlinearity – key assumptions
  - Saturated nonlinear state resembles linear mode structure
  - Mode saturates after growing by a factor of 10

Theorist’s post-processor

Computer Physics Communications *76* (1993) 3 18—327
Computer Physics
North-Holland
Communications
A post-processor for the PEST code
S. Preische, J. Manickam and J.L. Johnson
Princeton Plasma Physics Laboratory, Princeton University, Princeton, NJ 08543-0451, USA
Received 13 January 1992; in revised form 22 June 1992
A new post-processor has been developed for use with output from the PEST tokamak stability code. It allows us to use quantities calculated by PEST and take better advantage of the physical picture of the plasma instability which they can provide. This will improve comparison with experimentally measured quantities as well as facilitate understanding of theoretical studies.

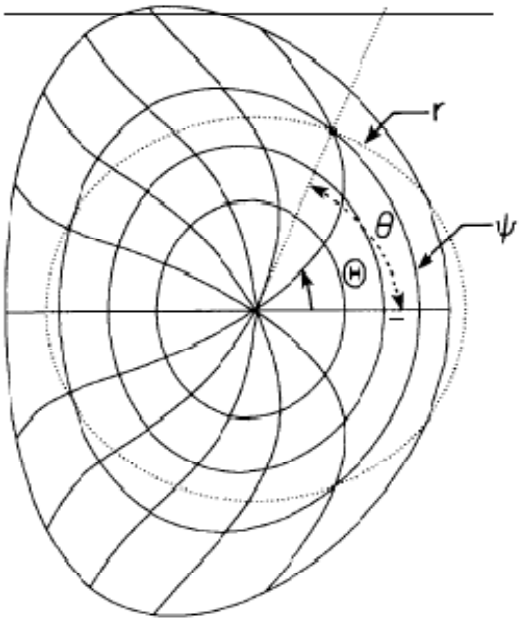

Fig. 1. Usual toroidal coordinates r, θ, ϕ compared with PEST coordinates ψ, Θ, ϕ. Solid lines show contours of constant ψ and Θ; dotted lines show usual r, θ coordinates for one point on the grid. Both systems use the same toroidal coordinate ϕ.

$$\xi = \frac{\mathcal{J}\xi_\psi^P}{gR^2}\nabla\Theta\times\boldsymbol{B} + \frac{\mathrm{i}\mathcal{J}\xi_S^P}{gR^2}\boldsymbol{B}\times\nabla\psi + \mathrm{i}\xi_B^P\boldsymbol{B}. \quad (3)$$

Fig. 1 compares the usual toroidal coordinate system with the PEST coordinate system, where Θ surfaces are chosen to enclose equal amounts of toroidal flux. Each component, α, of $\boldsymbol{\xi}$ has been decomposed such that

$$\xi_\alpha^P = \sum_{m,n}\xi_{\alpha,mn}^P(\psi)\,\mathrm{e}^{\mathrm{i}(m\Theta-n\phi)}. \quad (4)$$

Since axisymmetry is assumed, the Fourier coefficients for different values of n decouple from the major axis to the point (ψ, Θ)], have Θ dependencies so that graphs of these Fourier coefficients, $\xi_{\alpha,mn}^P$, without the appropriate normalization do not descibe the physical eigenfunctions.

2.2. Normalized components of ξ

To get a better physical picture of the Fourier modes of the displacement vector, we define a set of unit vectors

$$\boldsymbol{e}_\psi \equiv \frac{\nabla\Theta\times\boldsymbol{B}}{|\nabla\Theta\times\boldsymbol{B}|}, \quad \boldsymbol{e}_s \equiv \frac{\boldsymbol{B}\times\nabla\psi}{B|\nabla\psi|}, \quad \boldsymbol{e}_b \equiv \frac{\boldsymbol{B}}{B}, \quad (5)$$

write

$$\begin{aligned}\boldsymbol{\xi} &= \xi_\psi\boldsymbol{e}_\psi + \xi_s\boldsymbol{e}_s + \xi_B\boldsymbol{e}_b \\ &= \frac{\partial X}{2\pi gR^3}\left[R^2g^2|\nabla\Theta|^2 + f^2(\nabla\psi\cdot\nabla\Theta)^2\right]^{1/2}\xi_\psi^P\boldsymbol{e}_\psi \\ &\quad + \mathrm{i}\frac{\partial X|\nabla\psi|}{2\pi gR^3}\left[R^2g^2 + f^2|\nabla\psi|^2\right]^{1/2}\xi_s^P\boldsymbol{e}_s \\ &\quad + \frac{\mathrm{i}}{X}\left[R^2g^2 + f^2|\nabla\psi|^2\right]^{1/2}\xi_B^P\boldsymbol{e}_b, \end{aligned} \quad (6)$$

and Fourier decompose ξ_ψ, ξ_s, ξ_B in Θ. This set of Fourier coefficients is properly normalized and comparision of the relative amplitudes is meaningful.

2.3. Orthogonal projection of ξ

Since the PEST basis vectors are not orthogonal, i.e., $\nabla\psi\cdot\nabla\Theta \neq 0$, it is useful to look at $\boldsymbol{\xi}$ in an orthogonal system. To do this we define a new set of orthogonal unit vectors:

$$\boldsymbol{e}_r \equiv \frac{\nabla\psi}{|\nabla\psi|}, \quad \boldsymbol{e}_\Theta \equiv \frac{\boldsymbol{B}\times\nabla\psi}{B|\nabla\psi|}, \quad \boldsymbol{e}_b \equiv \frac{\boldsymbol{B}}{B}. \quad (7)$$

The perturbed fields are:

The most useful components of $\boldsymbol{Q}$ for experimental measurements are

$$Q_\psi = \frac{\boldsymbol{Q}\cdot\nabla\psi}{|\nabla\psi|}, \quad Q_\theta = \frac{\boldsymbol{Q}\cdot(\nabla\phi\times\nabla\psi)}{|\nabla\phi||\nabla\psi|},$$
$$Q_\phi = \frac{\boldsymbol{Q}\cdot\nabla\phi}{|\nabla\phi|}, \qquad (11)$$

where the component Q_θ now lies in a toriodal cross section. These components are

$$Q_\psi = \frac{1}{X^2|\nabla\psi|}\left\{\frac{2\pi f}{v}\frac{\partial\xi_\psi^P}{\partial\Theta} + g\frac{\partial\xi_\psi^P}{\partial\phi}\right\}, \qquad (12)$$

$$\begin{aligned} Q_\theta = &-\frac{|\nabla\psi|}{XR}\left[f\frac{\partial\xi_\psi^P}{\partial\psi} + \xi_\psi^P\frac{\partial f}{\partial\psi}\right] \\ &- \frac{f}{XR|\nabla\psi|}(\nabla\psi\cdot\nabla\Theta)\frac{\partial\xi_\psi^P}{\partial\Theta} \\ &- \frac{v^2}{4\pi^2 gR^3}\left[f^2|\nabla\psi|^2 + R^2g^2\right] \\ &\times\left[(\nabla\psi\cdot\nabla\Theta)\frac{\partial\xi_\psi^P}{\partial\phi} - \mathrm{i}|\nabla\psi|^2\frac{\partial\xi_s^P}{\partial\phi}\right], \qquad (13) \end{aligned}$$

$$\begin{aligned} Q_\phi = &\frac{f\xi_\psi^P}{X\bar{g}R^2}\left\{\frac{\partial}{\partial\psi}\left(\frac{f\mathcal{J}}{X^2}|\nabla\psi|^2\right)\right. \\ &\left.+\frac{\partial}{\partial\Theta}\left(\frac{f\mathcal{J}}{X^2}\nabla\psi\cdot\nabla\Theta\right)\right\} \\ &+\frac{f}{XR^2}|\nabla\psi|^2\frac{\partial}{\partial\psi}\left(\frac{f\xi_\psi^P}{g}\right) \\ &+\frac{f^2}{XgR^2}(\nabla\psi\cdot\nabla\Theta)\frac{\partial\xi_\psi^P}{\partial\Theta} \\ &-\frac{X}{\mathcal{J}R^2}\left\{\frac{\partial}{\partial\psi}\left(\frac{\mathcal{J}B^2\xi_\psi^P}{g}\right)\right. \\ &\left.+\mathrm{i}\frac{\partial}{\partial\Theta}\left(\frac{\mathcal{J}B^2\xi_s^P}{g}\right)\right\}. \end{aligned}$$

Perturbed fluid parameters(new)

The perturbed pressure is :

$$P_1 = -\gamma P \nabla \bullet \xi - \xi_r P' \left| \nabla \psi \right|$$

The perturbed density is :

$$\rho_1 = -\rho \nabla \bullet \xi - \xi_r \rho' \left| \nabla \psi \right|$$

The perturbed temperature is :

$$T_1 = \frac{P_1}{\rho} - \frac{P \rho'}{\rho^2}$$

Barely Unstable kink in NSTX

Eq profiles

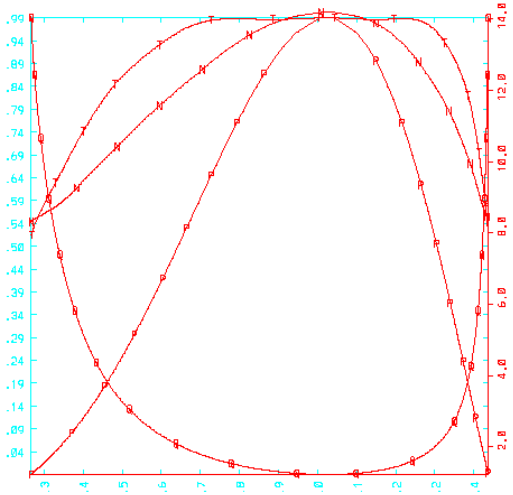

Fourier components

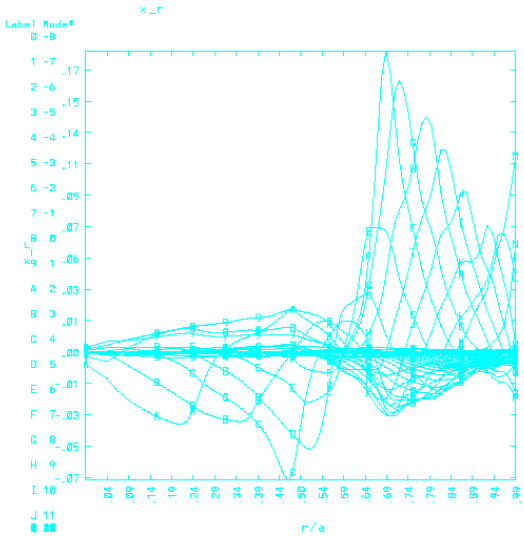

Displacement

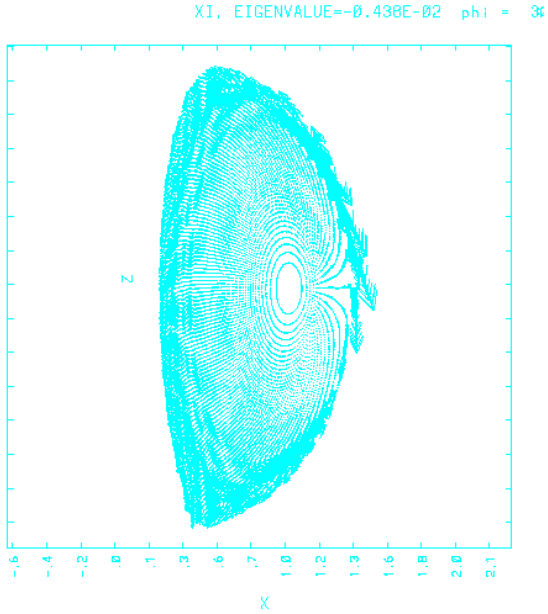

Data from experiment

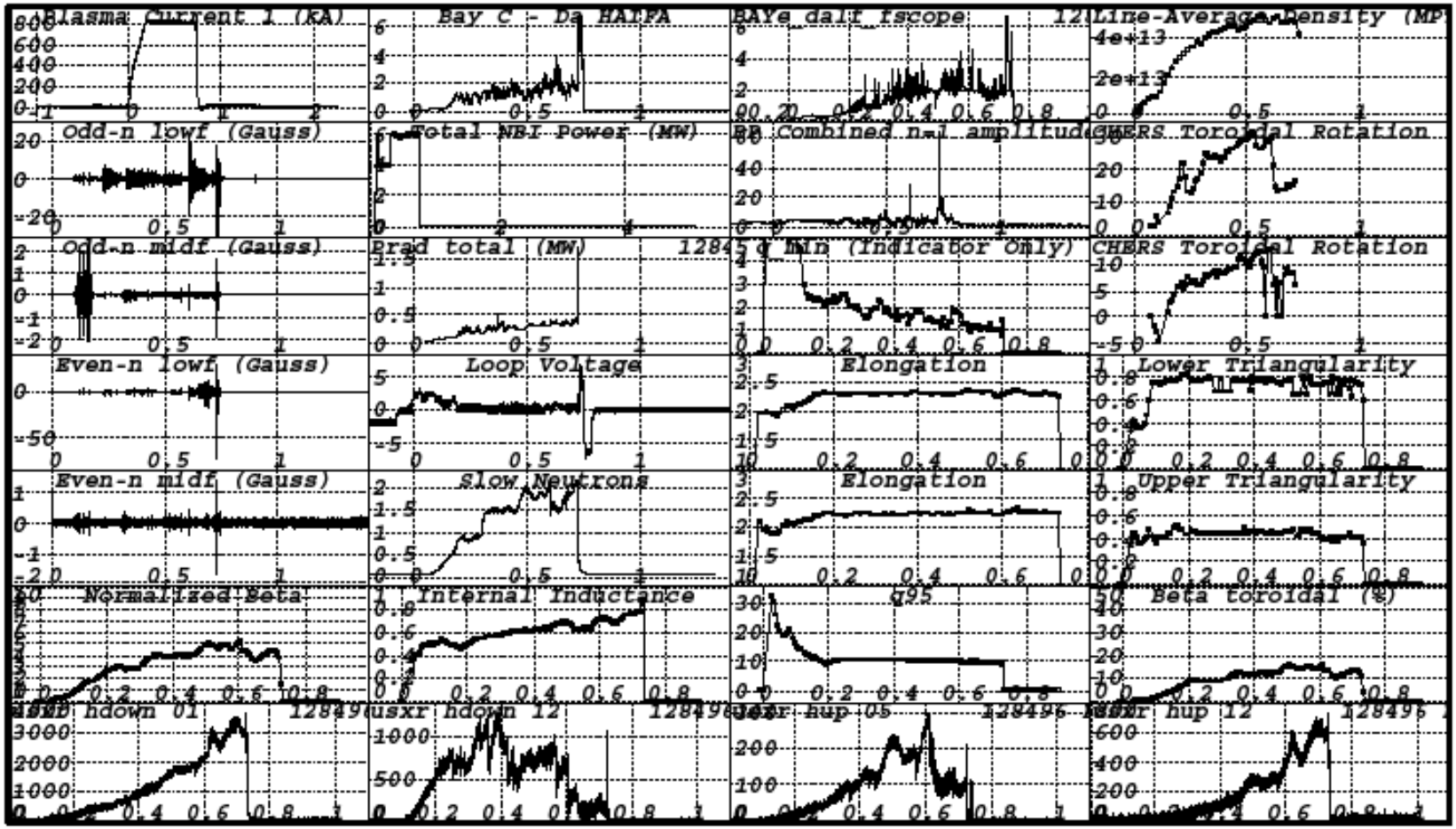

Equilibrium profiles and SXR sightlines

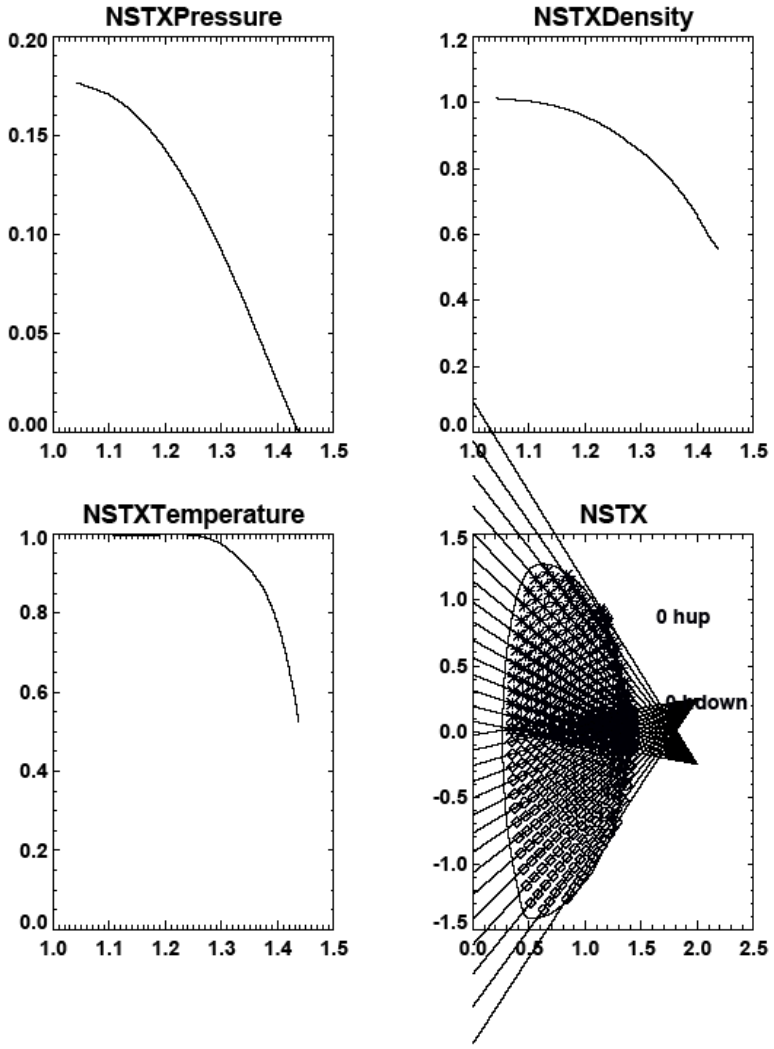

Soft X-ray emissivity

SIMULATION

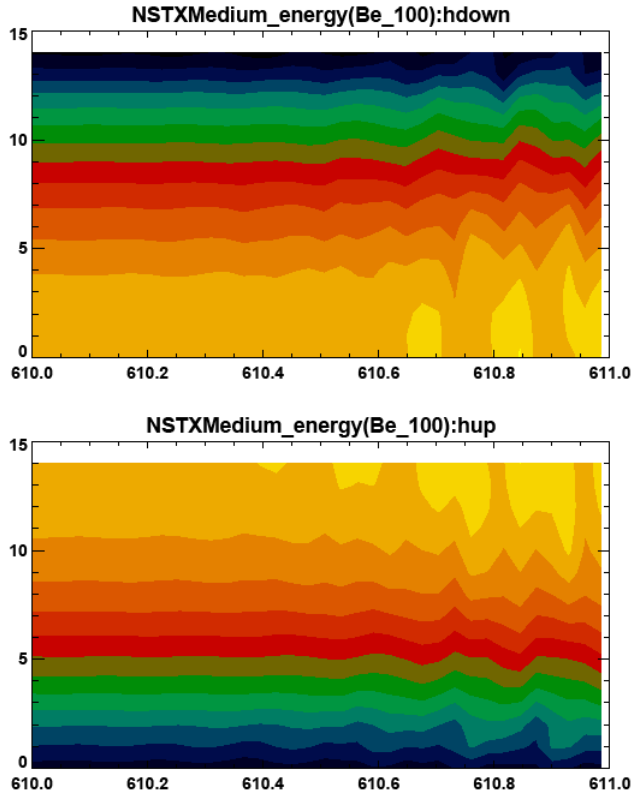

EXPERIMENT

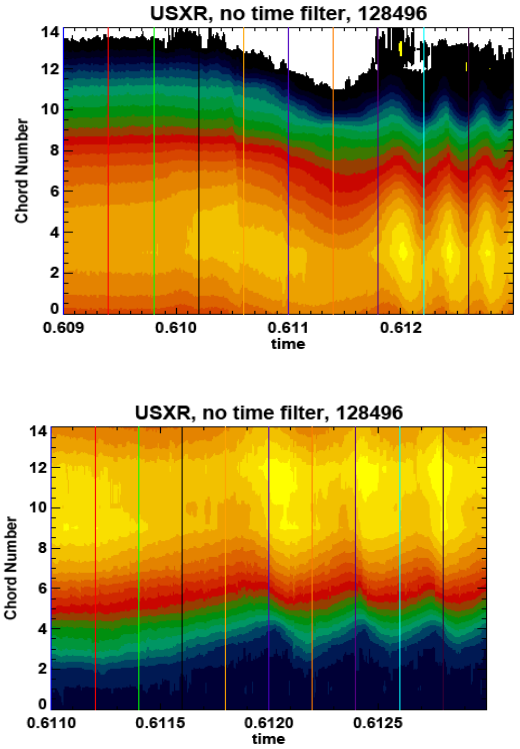

Simulated signals of SXR

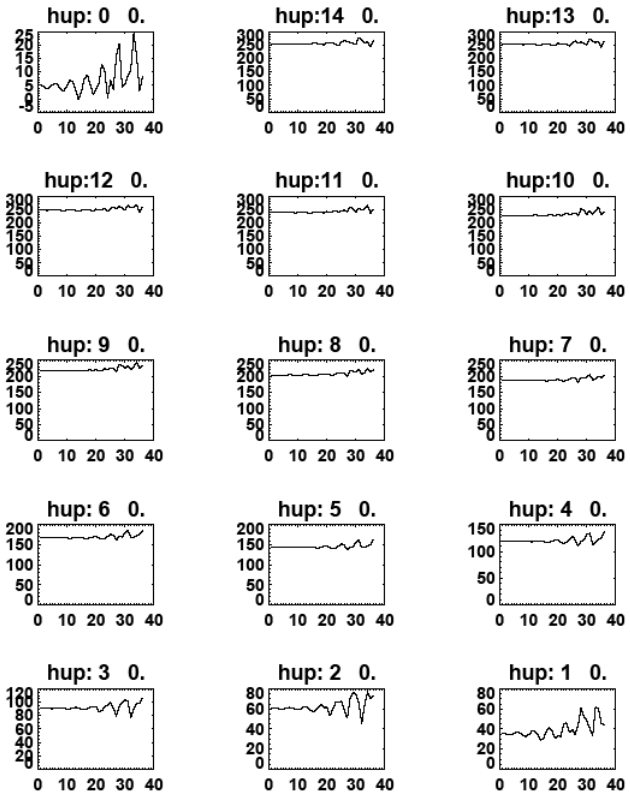

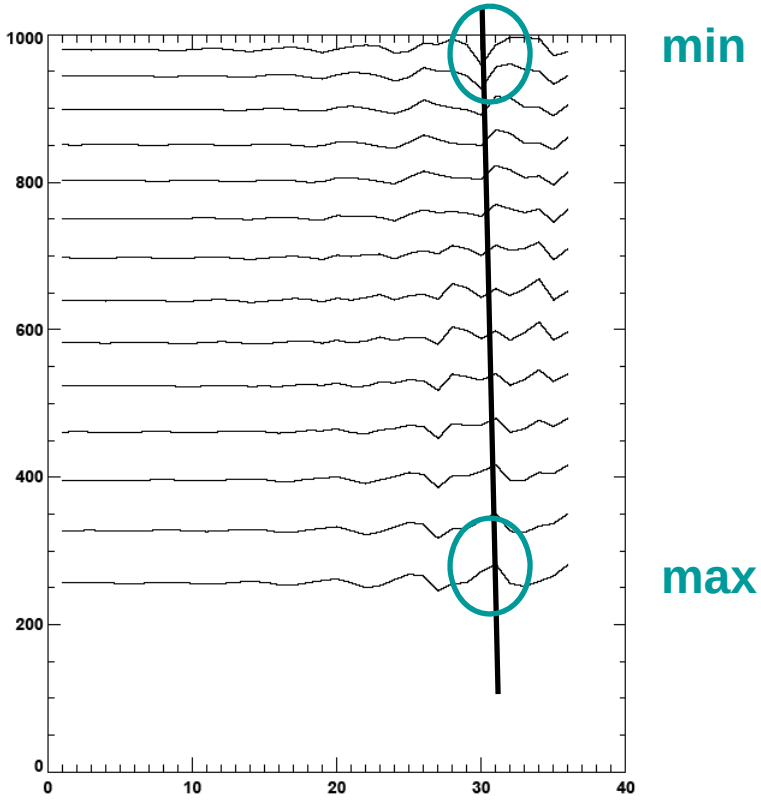

Berylium filters are simulated

SIMULATION

EXPERIMENT

No filter

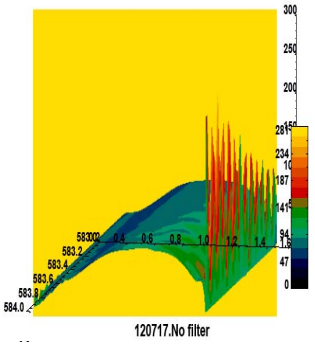

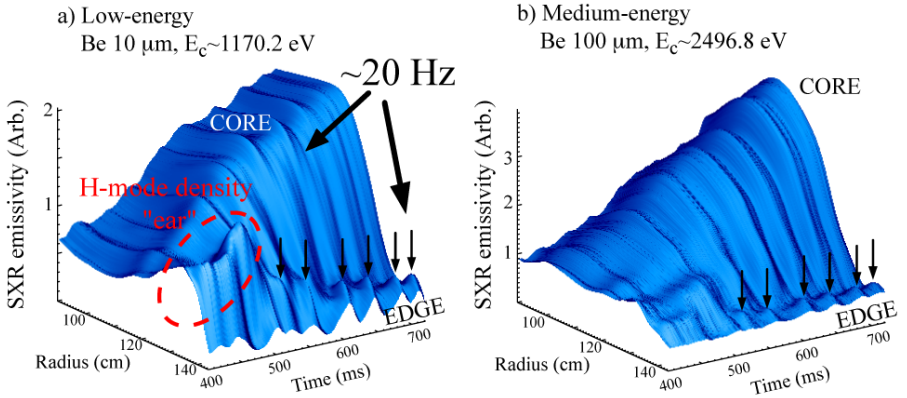

Low energy

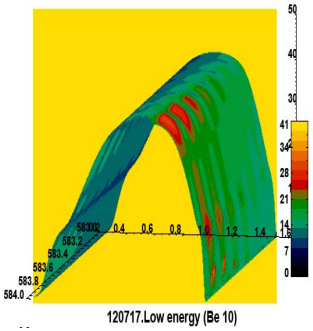

High energy

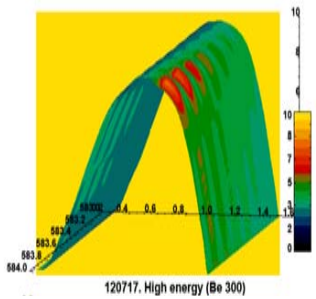

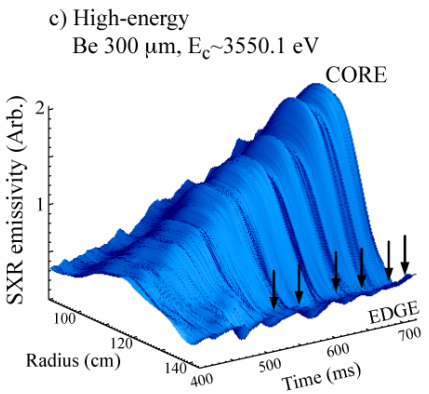

Perturbed field - MSE

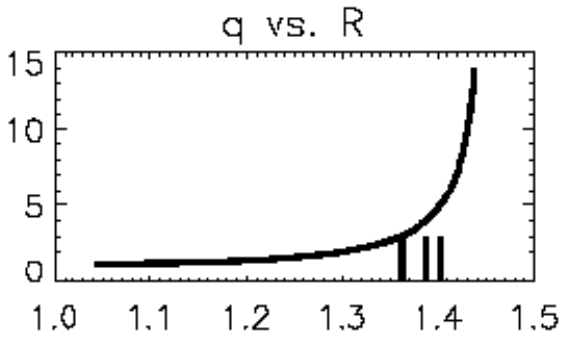

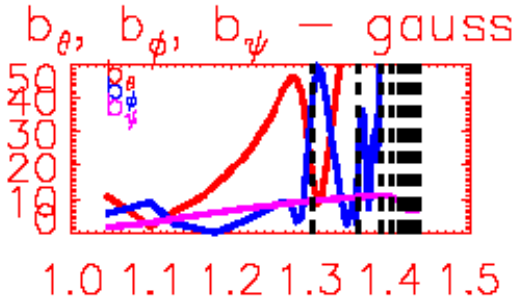

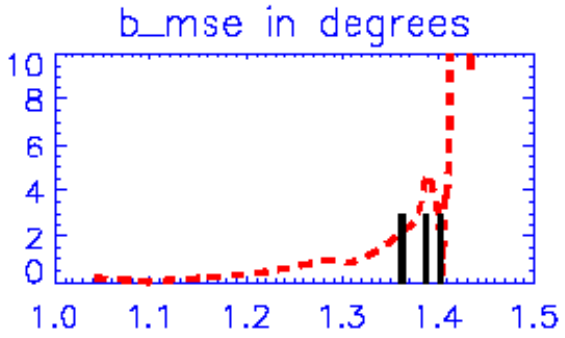

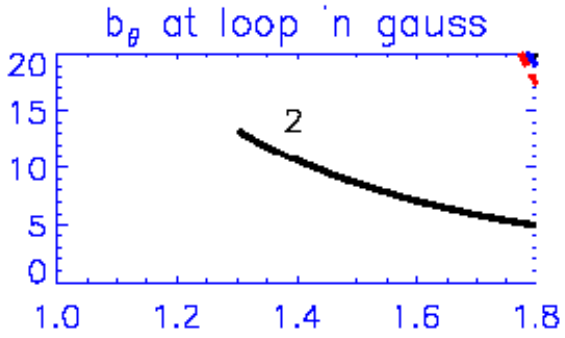

Simulation of ECE

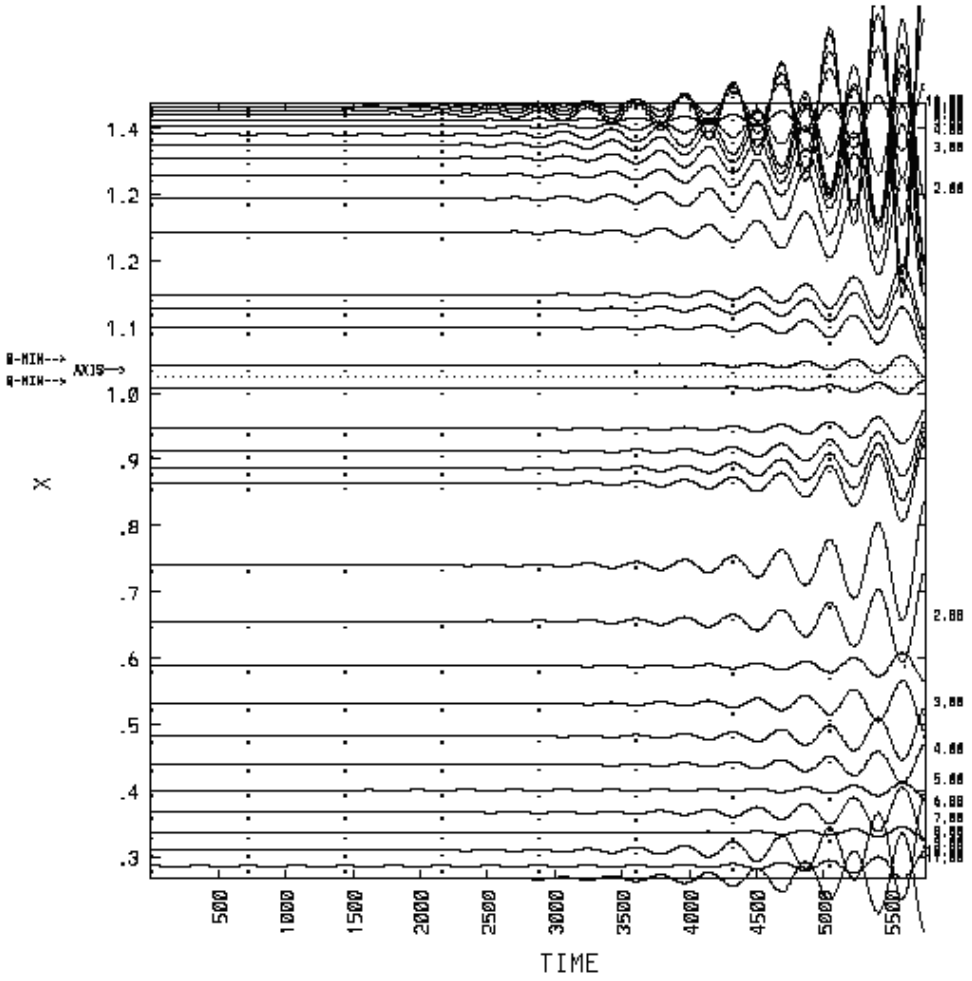

SUMMARY

- We have made significant progress towards developing a comprehensive suite of synthetic diagnostics
- ECE, Mirnov, MSE, SXR are ready for benchmarking
- FIRETIP under development
- Collaborators are welcome

Sign up sheet